Available online at www.eccomasproceedia.org
Eccomas Proceedia COMPDYN (2023) 5034-5040

ECCOMAS
Proceedia

COMPDYN 2023
9th ECCOMAS Thematic Conference on
Computational Methods in Structural Dynamics and Earthquake Engineering
M. Papadrakakis, M. Fragiadakis (eds.)
Athens, Greece, 12-14 June 2023

MODAL CHARACTERIZATION AND ROAD ROUGHNESS RECONSTRUCTION USING DYNAMIC VEHICLE ACCELERATIONS AND ANNS

Kais Douier[1], **Mohammed F. M. Hussein**[2], **and Jamil Renno**[3]

[1 2] Department of Civil and Architectural Engineering
Qatar University, Doha Qatar
e-mail: kd1204127@student.qu.edu.qa, mhussein@qu.edu.qa

[3] Department of Mechanical and Industrial Engineering
Qatar University, Doha Qatar
e-mail: jamil.renno@qu.edu.qa

Abstract

Road networks are considered huge and critical infrastructures that support the development and growth of societies. These infrastructures deteriorate over time due to regular usage and/or external environmental factors. Deteriorating road networks eventually cause ride discomfort for their users and the production of ground-borne noise and vibrations. Thus, maintaining these infrastructures is essential, and monitoring the condition of the roads is one of the most important steps in maintaining these road networks. Road roughness could be considered as one of the main indicators of the road's overall health. The International Roughness Index (IRI) is used to describe the road roughness profile numerically in a single value. Traditionally the IRI is obtained through manual or automated profilometers, profilographs, or dipstick profilers, which could be time/money consuming. Therefore, this study investigates the ability of Artificial Neural Networks (ANNs) in reconstructing road roughness profiles from dynamic vehicle accelerations. This study also investigates the ANNs ability to predict the model characteristics of a 7-DOF Full Car (FC) model, which is constructed to extract the dynamic vehicle accelerations of a vehicle moving on various roughness profiles. First, the FC model will be moving over a certain obstacle so that the developed ANN could take the dynamic vehicle accelerations as inputs and predict the FC model characteristics. Once the model characteristics are obtained, another ANN will be trained using the dynamic vehicle acceleration of an FC model with the same characteristics to reconstruct the road roughness profile.

Keywords: Artificial Neural Networks, Dynamic Vibrations, Modal Characterization, Road Roughness.

ISSN:2623-3347
Peer-review under responsibility of the organizing committee of COMPDYN 2023.
doi: 10.7712/120123.10780.21392

1 INTRODUCTION

The continuous measurement of road roughness levels is essential for maintaining the overall health and functionality of the road network. These levels provide a reliable indication of the road's ability to serve the public safely and efficiently. The ISO 8608 guidelines classify road roughness into eight categories, ranging from class A to class H, which describe the overall condition of a road section [1]. These roughness classes can also be assigned to road sections based on the International Roughness Index (IRI), which summarizes the road section's roughness profile into a single value [2]. Usually, the IRI is computed by utilizing a quarter-car model that travels on a road with a particular roughness level. Conventional manual and automated techniques, such as dipstick profilometer, profilograph, or automated road meters, are capable of determining the IRI of a road section[3]–[6]. Nonetheless, implementing these methods across an entire road network can be both expensive and time intensive.

Highway agencies and researchers have sought to find a more efficient method of monitoring road profiles by using specially designed trucks equipped with high-resolution cameras and lasers [7]–[11]. However, mounting such equipment on trucks requires significant capital and operational expenses, making it expensive compared to manual monitoring. Researchers have also explored using unmanned air vehicles (UAVs) to train artificial neural networks (ANNs) and convolutional neural networks (CNNs) to detect surface defects [12], [13]. Although these methods have the potential to be time and cost-effective, they lack the necessary accuracy to be integrated into highway management systems.

Boyu et al. [14] proposed a new technique for estimating road profiles using only a smartphone to measure the responses of an ordinary vehicle. They proposed a new algorithm that involves two main stages. Initially, the ordinary vehicle is modeled as a half car (HC), and a genetic algorithm (GA) is employed to identify its parameters by analyzing the vehicle's responses when it passes over a well-defined speed bump. Using the vehicle model that was estimated, a Kalman filter that incorporates the road profile as a part of the state vector is employed to estimate the road profile.

This research proposes the use of dynamic vehicle responses along with artificial neural networks (ANNs) to estimate road roughness profiles. A full car (FC) model will be developed for exporting the dynamic vehicle response of a normal car passing over randomly generated roughness profiles. The FC model will be also subjected to a road profile with a predefined speed bump to calibrate the model for road roughness estimations.

2 METHODOLOGY

This study aims towards reconstructing road roughness profiles using ANNs and dynamic vehicle responses. A numerical FC model will be used throughout this research. The FC model will be used to extract the vehicle dynamic responses to be later used for training the ANNs. Initially, the FC model with randomly varied parameters will be subjected to a predefined speed bump, from which the dynamic vehicle response will be used with ANN to calibrate the developed FC model. Then the calibrated FC model will be used with randomly generated roughness profiles to train another ANN in estimating the road roughness profile.

2.1 Full car (FC) model

This study utilizes a 7-degree-of-freedom (7-DOF) FC model that includes four unsprung masses on behalf of the vehicle's wheels and a single sprung mass representing the vehicle's body. The model also takes into account the pitch and roll of the vehicle's body as shown in Figure 1. Equations (1-15) [15], [16] provide a summary of the governing equations for the FC model.

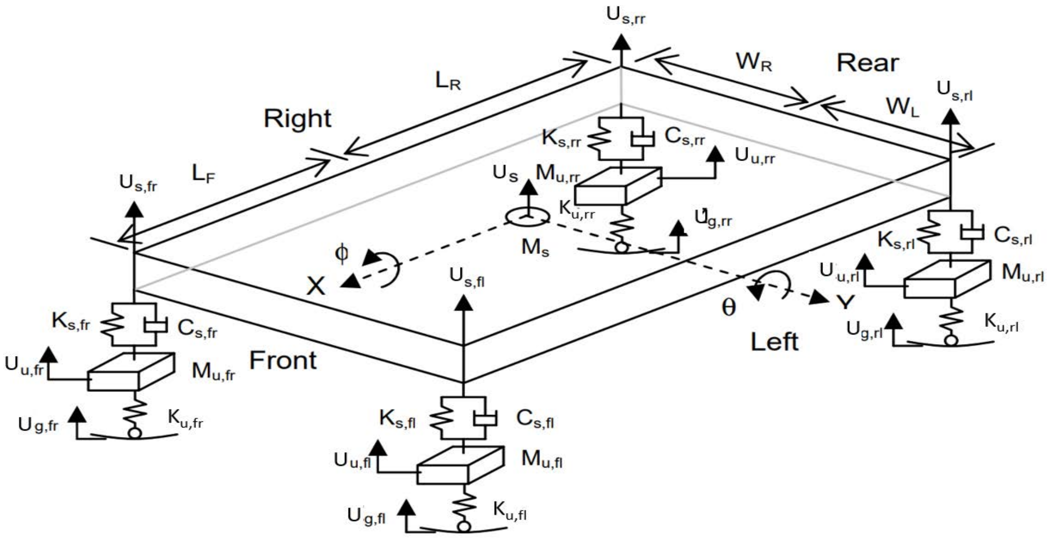

Figure 1: Full car model demonstration [14].

$$I_{yy}\ddot{\theta} = L_r\left(F_{s,rr} + F_{s,rl}\right) - L_f\left(F_{s,fr} + F_{s,fl}\right) \tag{1}$$

$$I_{xx}\ddot{\Phi} = W_l\left(F_{s,fl} + F_{s,rl}\right) - W_r\left(F_{s,fr} + F_{s,rr}\right) \tag{2}$$

$$F_{s,fr} = K_{s,fr}\left(U_{u,fr} - U_{s,fr}\right) + C_{s,fr}(\dot{U}_{u,fr} - \dot{U}_{s,fr}) \tag{3}$$

$$F_{s,fl} = K_{s,fl}\left(U_{u,fl} - U_{s,fl}\right) + C_{s,fl}(\dot{U}_{u,fl} - \dot{U}_{s,fl} \tag{4}$$

$$F_{s,rr} = K_{s,rr}\left(U_{u,rr} - U_{s,rr}\right) + C_{s,fl}(\dot{U}_{u,rr} - \dot{U}_{s,rr}) \tag{5}$$

$$F_{s,rl} = K_{s,rl}\left(U_{u,rl} - U_{s,rl}\right) + C_{s,rl}(\dot{U}_{u,rl} - \dot{U}_{s,rl}) \tag{6}$$

$$M_S\ddot{U}_S = F_{s,fr} + F_{s,fl} + F_{s,rr} + F_{s,rl} \tag{7}$$

$$M_{u,fr}\ddot{U}_{u,fr} = F_{u,fr} - F_{s,fr} \tag{8}$$

$$M_{u,fl}\ddot{U}_{u,fl} = F_{u,fl} - F_{s,fl} \tag{9}$$

$$M_{u,rr}\ddot{U}_{u,rr} = F_{u,rr} - F_{s,rr} \tag{10}$$

$$M_{u,rl}\ddot{U}_{u,rl} = F_{u,rl} - F_{s,rl} \tag{11}$$

where:

$$U_{s,fr} = U_s - L_f\theta - W_r\Phi \tag{12}$$

$$U_{s,fl} = U_s - L_f\theta + W_l\Phi \tag{13}$$

$$U_{s,rr} = U_s + L_r\theta - W_r\Phi \tag{14}$$

$$U_{s,rl} = U_s + L_r\theta + W_l\Phi \tag{15}$$

The equations listed above involve variables such as pitch angle (θ) and roll angle (Φ) that refer to the body of the vehicle and its corresponding mass moment of inertia Iyy and Ixx about the respective axes. The subscripts s, u, fr, fl, rr, and rl denote the sprung, unsprung, front right, front left, rear right, and rear left parts of the vehicle. Additionally, the terms L_f, Lr, Wr, and W_l refer to specific distances shown in Figure 1.

2.2 Levenberg-Marquardt ANNs

In this research, Levenberg-Marquardt ANNs are used to estimate the developed FC parameters and road roughness profiles. Compared to other techniques that require solving the Hessian matrix, the Levenberg-Marquardt method approximates it, which usually results in faster training of artificial neural networks.

The FC model parameter estimation ANN consisted of 387 input neurons containing the sprung mass accelerations, and the vehicle pitch and roll response. It also had 15 hidden tan sigmoidal neurons, with 6 linear output neurons corresponding to the roll and pitch moment of inertia, front and rear axles suspension stiffness, and front and rear axles suspension damping as shown in Figure 2 (a).

The road roughness estimation ANN consisted of 225 input neurons containing the sprung and unsprung masses' accelerations. It also had 20 hidden tan sigmoidal neurons, and 50 linear output neurons corresponding to the road profile in Figure 2 (b).

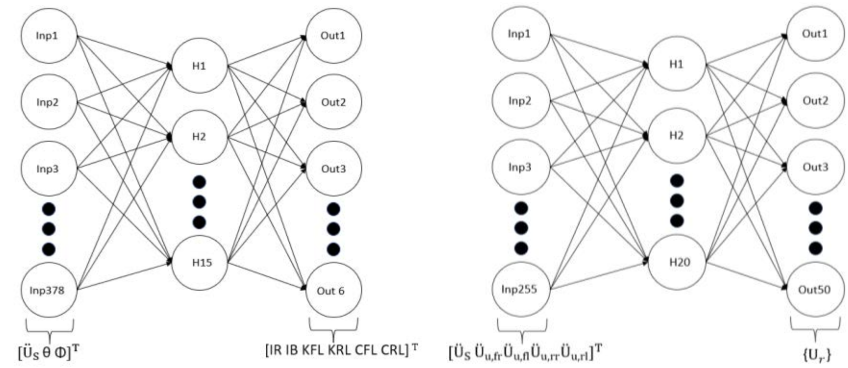

(a) (b)

Figure 2: ANN architecture.

2.3 Training Data Sets

The FC model parameter estimation ANN was trained by dynamic vehicle responses which were exported from the FC model moving over a predefined speed bump with a length of 1 m, and a height of 0.5 m. Figure 3 shows the front and rear left-wheel road profiles.

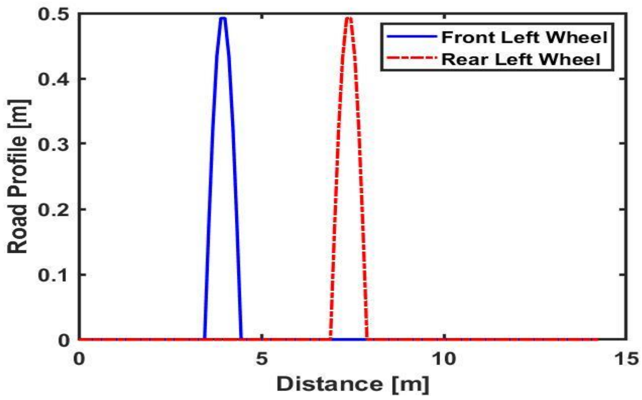

Figure 3: speed bump road profile.

A total of 3000 varied FC models were simulated moving over the above-mentioned speed bump. Each of the Varied FC models had a randomly assigned roll and pitch moment of inertia, front and rear axles suspension stiffness, and front and rear axles suspension damping. The ANN was later trained using the exported sprung mass accelerations, and the vehicle pitch and roll response as inputs, and the randomly assigned parameters as outputs. The vehicle sprung mass and the rear and front axle masses were fixed at 1500 and 60 kg, respectively. Also, the wheel stiffness for all four wheels was fixed at 190000 kN/m.

The road roughness estimation ANN was trained by the dynamic vehicle masses' accelerations which were exported from the calibrated FC model moving over various randomly generated roughness profiles. A total of 3000 randomly generated road roughness class C profiles were generated. The sprung and unsrpung mass accelerations were considered as inputs, while the randomly generated road roughness profiles were considered as outputs.

3 RESULTS AND DISCUSSION

Two separate ANNs were developed and tested in this research. The first ANN was used to calibrate the developed FC model, and the second ANN was used to estimate the road roughness profile. The randomly generated model parameters and the estimated model parameters with their error percentage are summarized in Table **1**. Also, the sprung mass acceleration of the true and estimated model parameters of an FC model passing over a speed bump is shown in Figure 4.

Parameters	True Values	Estimated Values	Percentage error (%)
Roll moment of Inertia (kg.m^2)	961.3	947.7	1.41
Pitch moment of Inertia (kg.m^2)	1970	1986.9	0.86
Front axle suspension stiffness (kN/m)	23000	22960	0.17
Rear axle suspension stiffness (kN/m)	19210	19242.3	0.17
Front axle suspension damping (kN s/m)	226.9	225	0.85
Rear axle suspension damping (kN s/m)	923.5	932.7	1.00

Table 1: True and estimated FC model parameters and their error percentages

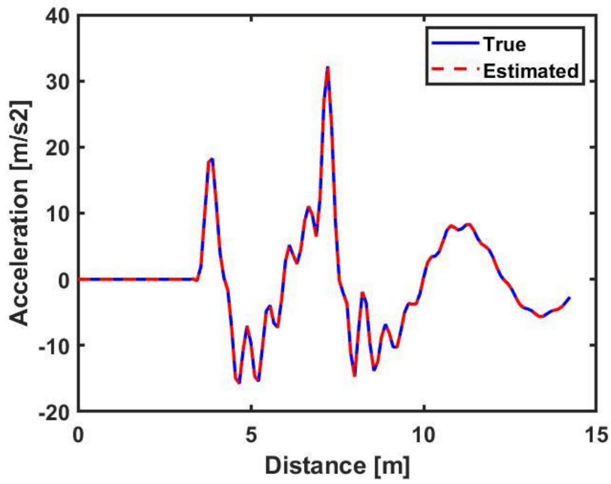

Figure 4: sprung mass acceleration of the true (solid blue) and estimated (dashed red) FC model.

Various runs were tried with randomly varying modal parameters. However, the model parameters were consistently estimated with less than 10% error. The resulting sprung mass acceleration of the estimated FC model showed great agreement with the true FC model, as shown in Figure 4.

The calibrated FC model was then used to train a different ANN to reconstruct the road roughness profile. The testing profile was comprised of 1000 data points that were randomly generated. Consequently, the reconstruction process of the roughness profile involved splitting it into 20 sections and utilizing the same ANN on each of the sections. Figure 5 (a) summarizes the true and estimated testing profile, while Figure (b) shows the regression between the two profiles. The road profile estimation ANN was able to reconstruct the road roughness profile with a regression of 0.94869 and a total root mean square error of 0.0064.

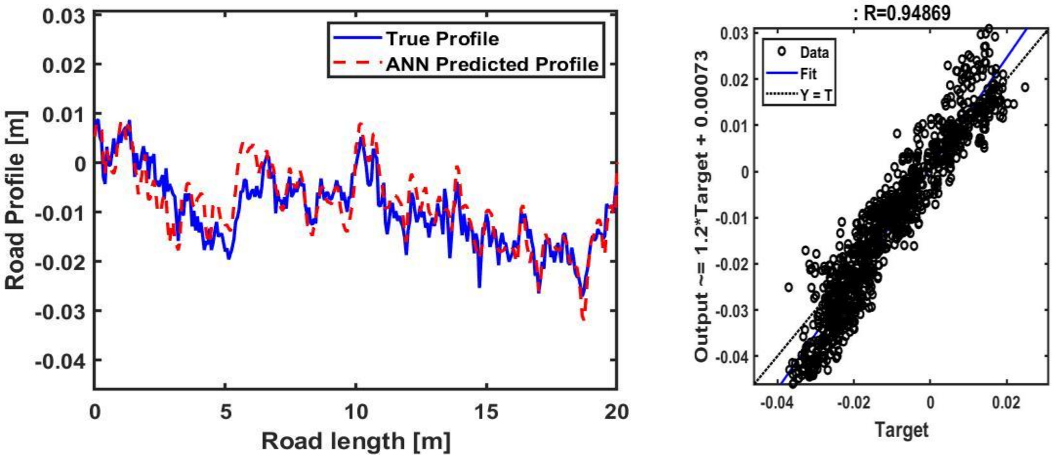

Figure 5: a) reconstructed (dashed red) and true (solid blue) road roughness profile, b) regression between the reconstructed and true roughness profiles.

4 CONCLUSION

The ability of ANNs to estimate the road roughness profile and FC model parameters was tested in this study. An FC model was subjected to a predefine speed bump, from which the sprung mass acceleration and the pitch and roll of the vehicle's body were used by a trained ANN to estimate the FC model's parameters. After this, the calibrated FC model was used to train a different ANN by subjecting the FC model to various randomly generated road profiles. The sprung and unsprung masses accelerations were exported from the FC model and utilized by the ANN to estimate the road roughness profile. Overall, both ANNs showed great potential in their ability to estimate unknown parameters such as the varied FC model parameters and randomly generated road roughness profiles.

5 ACKNOWLEDGMENT

The authors would like to acknowledge funding from Qatar University through a Graduate Assistantship. The authors would also like to acknowledge funding from Qatar Rail through grant number QUEX-CENG-QR-21/22-1.

REFERENCES

[1] I. 8608:2016(E), "INTERNATIONAL STANDARD ISO Mechanical vibration — Road surface profiles — Reporting of measured data," 2016.
[2] D. K. Singh and P. P. J. Gundaliya, "FLEXIBLE PAVEMENT," pp. 1024–1028, 2018.
[3] M. W. Sayers and S. M. Karamihas, "The little book of profiling," *Basic Inf. about Meas. Interpret. Road Profiles*, no. September, p. 100, 1998.
[4] A. Shtayat, S. Moridpour, B. Best, A. Shroff, and D. Raol, "A review of monitoring systems of pavement condition in paved and unpaved roads," *J. Traffic Transp. Eng. (English Ed.*, vol. 7, no. 5, pp. 629–638, 2020, doi: 10.1016/j.jtte.2020.03.004.
[5] M. J. Markow, "Highway Management Systems: State of the Art," *J. Infrastruct. Syst.*, vol. 1, no. 3, pp. 186–191, 1995.
[6] K. R. Benson, G. E. Elkins, W. Uddin, and W. R. Hudson, "Comparison of Methods and Equipment to Conduct Pavement Distress Surveys," 1999.
[7] L. Amador-Jimenez and N. Matout, "A low cost solution to assess road's roughness surface condition for Pavement Management," 2014.
[8] B. Becerik-Gerber, S. F. Masri, and M. R. Jahanshahi, "An Inexpensive Vision-Based Approach for the Autonomous Detection, Localization, and Quantification of Pavement Defects," *Innov. Deserving Explor. Anal.*, vol. 169, no. August, 2015.
[9] S. Sreedhar and E. Coleri, "The effect of long-term aging on fatigue cracking resistance of asphalt mixtures," *Int. J. Pavement Eng.*, vol. 0, no. 0, pp. 1–13, 2020, doi: 10.1080/10298436.2020.1745206.
[10] J. S. Miller and W. Y. Bellinger, "FHWA, Distress Identification manual for the Long-Term Pavement Performance Program. Report FHWA-HRT-13-092," 2014.
[11] H. E. M. Hunt and M. F. M. Hussein, "Ground-Borne Vibration Transmission from Road and Rail Systems: Prediction and Control," in *Handbook of Noise and Vibration Control*, M. J. Crocker, Ed. New York: John Wiley and Sons, 2007, pp. 1458–1469.
[12] C. Zhang and A. Elaksher, "An Unmanned Aerial Vehicle-Based Imaging System for 3D Measurement of Unpaved Road Surface Distresses," *Comput. Aided Civ. Infrastruct. Eng.*, vol. 27, pp. 118–129, 2012.
[13] M. Khoudeir, J. Brochard, V. Legeay, and M.-T. Do, "Roughness Characterization through 3D Textured Image Analysis: Contribution to the Study of Road Wear Level," *Comput. Civ. Infrastruct. Eng.*, vol. 19, no. 2, pp. 93–104, 2004, doi: https://doi.org/10.1111/j.1467-8667.2004.00340.x.
[14] B. Zhao, T. Nagayama, and K. Xue, "Road profile estimation, and its numerical and experimental validation, by smartphone measurement of the dynamic responses of an ordinary vehicle," *J. Sound Vib.*, vol. 457, pp. 92–117, 2019, doi: 10.1016/j.jsv.2019.05.015.
[15] K. M. Mahala, P. Gadkari, and A. Deb, "Mathematical Models for Designing Vehicles for Ride Comfort," *ICORD 09 Proc. 2nd Int. Conf. Res. into Des. Bangalore, India 07.-09.01.2009*, no. i, pp. 168–175, 2009.
[16] M. Saifuddin and M. Yusof, "Parametric Studies on Tramcar Suspension System," *1st Int. Conf. Nat. Resour. Eng. Technol.*, 2006.